# **Exploring Multimodal Large Language Models for Radiology Report Error-checking**

Jinge Wu<sup>1,\*,#</sup>, Yunsoo Kim<sup>1,\*,#</sup>, Eva C. Keller<sup>1</sup>, Jamie Chow<sup>1</sup>, Adam P. Levine<sup>2</sup>, Nikolas Pontikos<sup>3,4,5</sup>, Zina Ibrahim<sup>6</sup>, Paul Taylor<sup>1</sup>, Michelle C. Williams<sup>7</sup>, Honghan Wu<sup>1,#</sup>

- <sup>1</sup> Institute of Health Informatics, University College London, London, UK
- <sup>2</sup> Research Department of Pathology, University College London, London, UK
- <sup>3</sup> UCL Genetics Institute, University College London, London, UK
- <sup>4</sup> Institute of Ophthalmology, University College London, London, UK
- <sup>5</sup> Moorfields Eye Hospital, London, UK
- <sup>6</sup> Department of Biostatistics and Health Informatics, King's College London, London, UK
- <sup>7</sup> Centre for Cardiovascular Science, University of Edinburgh, Edinburgh, UK
- \*The authors have contributed equally.
- \*Corresponding Author: {jinge.wu.20, yunsoo.kim.23, honghan.wu}@ucl.ac.uk

#### Abstract

**Objective:** This paper proposes one of the first clinical applications of multimodal large language models (LLMs) as an assistant for radiologists to check errors in their reports.

**Methods:** We created an evaluation dataset from two real-world radiology datasets (MIMIC-CXR and IU-Xray), with 1,000 subsampled reports each. A subset of original reports was modified to contain synthetic errors by introducing three types of mistakes: "insert", "remove", and "substitute". The evaluation contained two difficulty levels: SIMPLE for binary error-checking and COMPLEX for identifying error types. LLaVA (Large Language and Visual Assistant) variant models, including our instruction-tuned model, were used for the evaluation. Additionally, a domain expert evaluation was conducted on a small test set.

**Results and Discussion:** At the SIMPLE level, the LLaVA v1.5 model outperformed other publicly available models. Instruction tuning significantly enhanced performance by 47.4% and 25.4% on MIMIC-CXR and IU-Xray data, respectively. The model also surpassed the domain expert's accuracy in the MIMIC-CXR dataset by 1.67%. Notably, among the subsets (N=21) of the test set where a clinician did not achieve the correct conclusion, the LLaVA ensemble mode correctly identified 71.4% of these cases. However, all models performed poorly in identifying mistake types, underscoring the difficulty of the COMPLEX level.

**Conclusion:** This study marks a promising step toward utilizing multi-modal LLMs to enhance diagnostic accuracy in radiology. The ensemble model demonstrated comparable performance to clinicians, even capturing errors overlooked by humans. Nevertheless, future work is needed to improve the model's ability to identify the types of inconsistency.

#### INTRODUCTION

Clinical reports, encompassing a wide range of medical documentation, are essential in patient care for recording diagnoses, treatments, and patient outcomes. Radiology reports, a critical subset of clinical reports, provide detailed interpretations of medical imaging studies such as X-rays, CT scans, and MRI scans. Their accuracy directly influences clinical diagnosis and subsequent patient care decision-making. The complexity and importance of these reports are highlighted in the medical literature, underscoring the need for precision and clarity in their formulation (1-2). This precision is not only critical for diagnosing acute conditions but also for guiding long-term treatment plans for complex and chronic illnesses such as cancer (3).

The advent of advanced natural language processing (NLP) techniques, notably large language models (LLMs) like the GPT series (4-7), could bring a transformative change in how clinical reports are generated and utilized. These models, capable of automated report generation and summarization, mark a significant leap forward in medical informatics. For example, Zhang et al. (8) proposed a machine learning method for radiology report summarization tasks. Another study proposed a pre-constructed graph embedding module to assist the generation of reports (9).

More recently, the field has begun to explore multi-modal applications, as highlighted in research by Xue et al. (10). This emerging area focuses on integrating visual data, such as radiological images, with textual analysis to generate more comprehensive and accurate clinical reports. This approach exemplifies the growing trend in medical AI to synergize different data modalities for improved patient care and report accuracy.

However, despite their potential, the application of these models, particularly in specialized fields like radiology, comes with significant challenges. It has been noted that original clinical reports authored by clinicians can sometimes contain errors (11). These inaccuracies, though often subtle, can be human-derived and system-derived, would have far-reaching implications. In particular, errors in clinical reports can lead to misinformed decision-making, potentially compromising patient safety (12). Moreover, when such reports are used as training data for models, these errors are inadvertently learned and perpetuated by the model, thus undermining the reliability of the models. Therefore, identifying and rectifying these errors is crucial for ensuring the accuracy and dependability of both the clinical reports and the models trained on them. Another critical challenge arises from the models' reliance on textual data. The recent study introduces a benchmark for error-checking in radiology reports, yet its exclusive focus on the reports themselves deviates significantly from real-world situations (13). Radiology inherently involves complex imaging data, which these text-centric models might struggle to interpret and correlate with clinical contexts accurately. Such gaps in interpretation can lead to serious errors in patient care, including incorrect diagnoses and inappropriate treatment recommendations. Therefore, the adoption of a multimodal approach in report auditing is important, as it bridges the gap between text-based analysis and the nuanced understanding of imaging data, ensuring a more accurate and holistic evaluation of patient information.

To address current challenges in clinical accuracy, we propose an innovative error-checking methodology that combines textual and imaging data (Figure 1). This approach is crucial for improving clinical practice by ensuring the reliability of radiology reports. Our method involves the creation of a unique dataset, where radiology reports are modified to simulate real-world errors. Pinpointing errors or inconsistencies in existing reports with multimodal LLMs is beneficial in assisting clinicians in verifying the quality of reports.

By employing cutting-edge vision-language models for evaluation, our approach establishes a pioneering standard in the evaluation of multi-modal clinical tasks. This advancement is instrumental in propelling the application of multimodal language models within specialized domains, such as radiology. Furthermore, to better conduct this task, we fine-tuned the open domain multimodal LLM, LLaVA 1.5 model (20) with a clinical error-checking instruction tuning dataset. The instruction-tuned model showed its effectiveness and improvement on this task, which can better serve as an assistant for radiologists to check for errors in their reports.

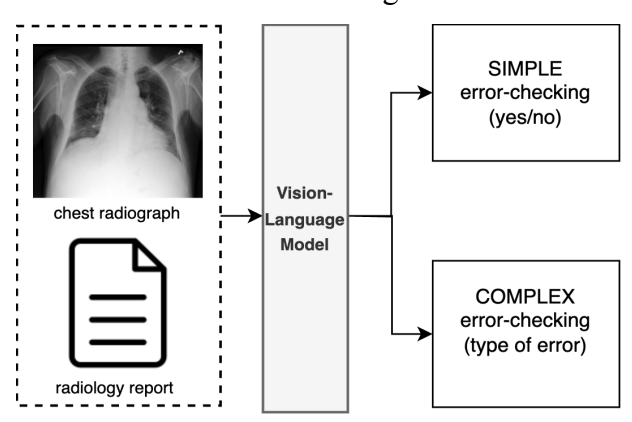


Figure 1. Error-checking task description.

#### **MATERIALS AND METHODS**

#### **Evaluation data creation**

We used chest radiology studies collected from MIMIC-CXR (14) and IU-Xray (15). The MIMIC-CXR data includes 371,110 chest X-rays and 227,835 chest radiology reports performed at the Beth Israel Deaconess Medical Center in Boston, MA between 2011-2016. This means one radiology report can be associated with multiple images in different views, such as anterior to posterior (AP), posterior to anterior (PA), and Lateral. As PA is considered the standard view, we used only PA X-rays. For each report, we only use the "findings" section, which is the description written by a radiologist, and paired this with the corresponding X-ray image.

IU-Xray originates from the Indiana University School of Medicine. The original data contains 7,470 images with 3,955 reports. We used the same approach to filter the original data and obtained 3,199 PA images with "findings" from the reports.

We use the entity retrieval toolkit, SemEHR (16), specifically tailored for analyzing clinical reports. This tool is designed to identify clinical concepts embedded within the reports. Following the automated identification process, we asked expert radiologists to select and rank the clinical concepts that are quintessential for radiographic studies. Based on this, the evaluation data for error-checking was created by modifying the original report (N) with three types of mistakes on mentions of those top 30 expert-ranked most important concepts:

1) "substitute" mistake (**W**): to randomly replace important concepts with other irrelevant ones. Figure 2 shows the modified report with the "substitute" mistake, where we replaced the original concept "atelectas" with "calcinoses".

- 2) "insert" mistake (I): to add an irrelevant sentence to the original report. In Figure 2, there is an example illustrating our evaluation data. For the "insert" mistakes, we added a fake sentence "Hyperemia indicates a foreign body in the right subclavian".
- 3) "remove" mistake (**R**): to randomly remove a sentence with important concepts from the original report. Figure 2 shows that red text with strikethrough shows the removed sentence.

Original report	"substitute" mistake	"insert" mistake	"remove" mistake
Single lead pacemaker is	Single lead pacemaker is	Single lead pacemaker is	Single lead pacemaker is
unchanged with lead	unchanged with lead	unchanged with lead extending	unchanged with lead
extending to the region of	extending to the region of	to the region of the right	extending to the region of the
the right ventricle. Again	the right ventricle. Again	ventricle. Again noted, is a	right ventricle. Again noted, is
noted, is a large right	noted, is a large right	large right pleural effusion.	a large right pleural effusion.
pleural effusion.	pleural effusion.	Associated compressive	Associated compressive
Associated compressive	Associated compressive	atelectasis in the right middle	atelectasis in the right middle
atelectasis in the right	calcinoses in the right	and lower lobes is again seen.	and lower lobes is again seen.
middle and lower lobes is	middle and lower lobes is	Hyperemia indicates a	Left lung is essentially clear
again seen. Left lung is	again seen. Left lung is	foreign body in the right	without large effusion or focal
essentially clear without	essentially clear without	subclavian. Left lung is	consolidation. Mild
large effusion or focal	large effusion or focal	essentially clear without large	interstitial edema is present.
consolidation. Mild	consolidation. Mild	effusion or focal consolidation.	The heart remains enlarged.
interstitial edema is	interstitial edema is	Mild interstitial edema is	No pneumothorax.
present. The heart remains	present. The heart remains	present. The heart remains	
enlarged. No	enlarged. No	enlarged. No pneumothorax.	
pneumothorax.	pneumothorax.		

**Figure 2.** Example of a report with each type of mistake. Red texts indicate the synthetic mistakes that are introduced in the original report.

Our evaluation dataset comprises a mix of original and erroneous reports, as outlined in Table 1 which details the data quantity and report lengths. We selected 1,000 reports from both the IU-Xray and MIMIC-CXR datasets. Approximately 75% of these are original reports, while the remaining 25% contain various types of errors, with each featuring only one mistake. More detailed statistics are given in Table 1. This approach aims to mirror real-world scenarios where only a minority of reports are expected to have errors. The dataset selectively includes a greater number of reports featuring substitute errors, anticipating their higher occurrence in real-world scenarios. All reports were chosen through random sampling to ensure a representative selection. In terms of report length, IU-Xray reports are, on average, about 100 words shorter than those from MIMIC-CXR (Table 1).

**Table 1.** Evaluation data description. The sample size and length of reports are described. N - original report, W - reports with "substitute" mistake, I - reports with "insert" mistake, R - reports with "remove" mistake. The total sample size and average length of reports are provided as well.

	Sample size					Leng	th of rej	ports		
Dataset	Total.	N	W	I	R	Avg.	N	W	I	R
IU-Xray	1,000	743	99	74	84	209	206	233	243	171
MIMIC -CXR	1,000	756	101	76	67	302	302	294	235	376

# **Error-checking problem definition**

The primary task revolves around examining chest Xray alongside its corresponding report to determine the presence of errors. Notably, the challenge extends beyond mere identification to encompass categorization, requiring the model to not only confirm the existence of errors but also classify the specific type of error or discrepancy within the report. The evaluation framework is structured with two levels of difficulty:

#### SIMPLE level

The model is tasked with determining if there is any error between the input chest X-ray report findings and the corresponding frontal view image. The expected responses are binary, with "Y" indicating the presence of inconsistency and "N" indicating no inconsistency.

## **COMPLEX** level

Beyond merely identifying the existence of error, the model in this setting also categorizes the type of error detected. The categorization includes "W" for instances where an important concept was replaced, "R" for the removal of a phrase or sentence, and "I" for the insertion of a phrase or sentence.

This two-level design aims to comprehensively evaluate the model's ability in error-checking, from simple binary assessments to nuanced identification and categorization of different types of mistakes in radiological reports.

#### SHARED SYSTEM MESSAGE

You are a senior radiologist and expert in chest xray report. Always answer accurately and precisely. If a question does not make any sense, or is not factually coherent, explain why instead of answering something not correct. If you don't know the answer to a question, please don't share false information. Below is an instruction that describes a task, paired with an input that provides further context. Write a response that appropriately completes the request.

#### **SIMPLE**

### Instruction:

Your junior radiologist made a report with the following findings about the chest xray image. You need to verify if there is any mistakes or fact inconsistency in findings. Answer with the option's letter from the given choices directly: 'N' - no mistakes or no fact inconsistency in findings, 'Y' - mistakes or fact inconsistency in findings.

### Findings: {findings}

### Response:

#### **COMPLEX**

### Instruction:

Your junior radiologist made a report with the following findings about the chest xray image. You need to verify if there is any mistakes or fact inconsistency in findings. Answer with the option's letter from the given choices directly: 'N' - no mistakes or no fact inconsistency in findings, 'W' - used a wrong word in findings, 'I' - inserted a irrelevant sentence in findings, 'R' - removed a relevant sentence in findings.

### Findings: {findings}

### Response:

**Figure 3.** SIMPLE and COMPLEX level prompt template.

#### **Models**

LLaVA is the first model that used a visual instruction dataset to train a LLM into a vision-language model (19). We selected the following three LLaVA models as baseline models and compared the performance of the evaluation datasets with our instruction-tuned model.

**LLaVA-0:** LLaVA is one of the pioneering multimodal LLMs. The model weight we used is the early version of LLaVA that combines a vision encoder and Vicuna, which is LLaMA trained for instruction purposes, for general-purpose visual and language understanding (17). The model is trained with visual instruction tuning techniques, demonstrating its powerfulness when presented

with unseen images and instructions. We will call this model LLaVA-0 hereafter. We used the 7B model.

**LLaVA-Med:** LLaVA-Med is one of the first multimodal foundational models in the biomedical domain (21). LLaVA-Med is initialized with LLaVA-0 and then continuously trained with a comprehensive dataset of biomedical figure-caption pairs sourced from PubMed Central. Only the 7B model is available publicly.

**LLaVA-1.5:** LLaVA-1.5 is a general domain vision-language model that uses the LLaMA2 model, which has a significant improvement in language understanding when compared with LLaMA, as the backbone LLM (18,20). There are two significant improvements besides the change of the backbone LLM. Firstly, the addition of an MLP vision-language connector enhanced the system's capabilities. Secondly, the integration of academic task-oriented data further enhanced its performance and effectiveness. We used the 7B model.

**LLaVA-CXR:** We fine-tuned **LLaVA-1.5** with the MIMIC-CXR error-checking instruction tuning dataset. The fine-tuning dataset was constructed using 17,000 MIMIC-CXR X-rays and reports. We prepared this dataset in the same way as the evaluation dataset, except we included the expected response from the model. The response of the model was restricted to either "Y" or "N" as a binary error-checking task. We introduced mistakes in 8,492 reports, leaving 8,508 reports unchanged. Each type of mistake was introduced in equal proportion. We ensured there was no data leakage (overlap between the instruction tuning dataset and the evaluation dataset). The fine-tuning code was obtained from LLaVA's official GitHub page (20). Due to GPU resource limitation, we used several techniques such as LoRA, ZeRO3, and Flash Attention to reduce the GPU memory requirement (22-24). We used the same hyperparameter settings as per the LLaVA guidance on GitHub for task-specific fine-tuning, except for reducing the training batch size to 8 and the number of epochs to 2.

# **Prompting strategy**

In leveraging the LLaVA models, we explored two prompting strategies: zero-shot and in-context learning (few-shot), recognizing the pivotal role that these strategies play in shaping the models' responses. By utilizing zero-shot learning, we sought to assess the model's innate understanding of radiographs and reports by generating accurate responses without the provision of specific examples (shots). Zero-shot learning prompt template is shown in Figure 3. In-context learning, which is widely accepted to improve the performance of LLMs, was conducted to assess the model's learning ability based on provided examples. We provided two shots for the SIMPLE setting and four shots for the COMPLEX setting to ensure one example per choice is provided. We further conducted an ablation study to identify the optimal learning capacity with varying numbers of shots from 0 to 10.

#### **Evaluation**

For evaluation, the temperature and the number of output tokens were constrained to 0 and 1 respectively. This setting ensures consistent and predictable outputs. The evaluation metric is F1 for both levels of difficulty. For the calculation of the F1 score, we treated reports with mistakes as positive regardless of the type of the mistake.

For the most effective model with in-context learning capacity at 2-shot and 4-shot prompting strategy setting, we undertook a comprehensive analysis to understand the impact of the increase in the number of examples (shots), ranging from 0 to 10, with 10 repetitions for each shot. This evaluation allowed us to determine the optimal shot number for best performance.

#### **Human Evaluation**

Two clinicians evaluated a random selection of 60 samples drawn from the MIMIC and IU X-ray datasets, with 30 samples from each. Within the dataset, 16 samples were selected for each type of mistake, totaling 48 mistakes, while the remaining 12 reports were 'original.' Given the change in the dataset's mistake proportion, accuracy was chosen as the metric instead of the F1 score. We also limited the difficulty of the task to be SIMPLE.

# **Comparing Human Answers with Model Answers**

We used the model's result from zero-shot prompting strategy to mirror the conditions faced by clinicians who did not have examples shown to them for their analysis.

#### RESULTS

#### **Zero-shot Evaluation**

Table 2 shows that instruction tuning within the medical domain enhanced the LLaVA variant models' inherent ability to perform the error-checking task in the SIMPLE setting. Specifically, LLaVA-Med was better than its backbone model LLaVA-0 by 20.61 in MIMIC-CXR and by 21.03 in IU-Xray. Likewise, the performance of LLaVA-CXR surpassed its baseline model, LLaVA-1.5, by 47.39 in MIMIC-CXR and 25.40 in IU-Xray, positioning LLaVA-CXR as the top-performing model for the SIMPLE difficulty level.

However, all LLaVA models, including the fine-tuned models, performed poorly in the COMPLEX setting. Despite this, LLaVA-0 was the best-performing model for MIMIC-CXR and LLaVA-Med was the best model for IU-Xray datasets.

**Table 2.** Zero-shot Evaluation Result. The best result is bolded for each task.

	MIMIC-CXR		IU-Xray	
Model	SIMPLE(F1)	COMPLEX(F1)	SIMPLE(F1)	COMPLEX(F1)
LLaVA-0	12.91	3.36	8.61	0.00
LLaVA-Med	33.52	0.40	29.64	4.91
LLaVA-1.5	35.79	0.00	40.60	0.00
LLaVA-CXR	83.18	0.00	66.00	0.00

The comparative assessment in Table 2 reveals that LLaVA-1.5 outperformed LLaVA-Med in both datasets, highlighting the importance of the backbone LLM. This is also confirmed by qualitative analysis (Figure 4). Figure 4 shows an example of a "remove" mistake and the responses from all four models. Both LLaVA-0 and LLaVA-Med gave a response of "Based", which is clearly irrelevant given the prompt (as detailed in Figure 3). The example also shows that all the models got a wrong answer for the COMPLEX difficulty, while LLaVA-1.5 and LLaVA-CXR yielded correct responses for the SIMPLE difficulty. It's worth noting that LLaVA-CXR, while also producing an irrelevant answer, may be constrained by the current instruction tuning dataset, which only allows for a binary "Y" or "N" response.

# Findings with "remove" mistake

Single lead pacemaker is unchanged with lead extending to the region of the right ventricle. Again noted, is a large right pleural effusion. Associated compressive atelectasis in the right middle and lower lobes is again seen. Left lung is essentially clear without large effusion or focal consolidation. Mild interstitial edema is present. The heart remains enlarged. No pneumothorax.

LLaVA-0		LLaVA-Med		LLaVA-1.5		LLaVA-CXR	
SIMPLE	COMPLEX	SIMPLE	COMPLEX	SIMPLE	COMPLEX	SIMPLE	COMPLEX
"Based"	"Based"	"Based"	"I"	"Y"	"N"	"Y"	"Y"

**Figure 4.** Qualitative analysis of one sample. The result is sampled from the zero-shot evaluation result.

# **Exploration of In-context Learning**

The effect of in-context learning, which is known to improve the performance of a LLM, is shown in Table 3, where 2-shot and 4-shot learning were conducted for SIMPLE and COMPLEX respectively. The performance boost in LLaVA-0 for IU-Xray at SIMPLE difficulty was the highest, +29.55, while the performance decrease in LLaVA-Med for MIMIC-CXR at SIMPLE difficulty was the largest, -30.48. LLaVA-CXR also suffered from a performance decrease in the IU-Xray SIMPLE task. Table 3 shows that LLaVA-1.5 is the only model where providing examples of each choice does not decrease the performance of the model in all difficulties and datasets. On the other hand, LLaVA-Med was the only model that performed worse with in-context learning in all difficulties and datasets. We chose LLaVA-1.5, the best-performing in-context learning model, for the further ablation study.

**Table 3.** In-context learning Evaluation Result. 2-Shot, and 4-Shot examples were provided for simple and complex tasks respectively. The best result is bolded for each task. Also, the performance change from the zero-shot evaluation result is provided in parenthesis.

	MIMIC-CXR		IU-Xray		
Model	SIMPLE (F1)	COMPLEX (F1)	SIMPLE (F1)	COMPLEX (F1)	
LLaVA-0	8.53(-4.38)	3.36(-2.15)	38.16(+29.55)	0.00(+0.00)	
LLaVA-Med	3.04(-30.48)	0.20(-0.20)	19.91(-9.73)	0.74(-4.91)	
LLaVA-1.5	40.10(+4.31)	0.00(+0.00)	<b>47.39</b> (+6.79)	<b>4.53</b> (+4.53)	
LLaVA-CXR	<b>83.29</b> (+0.11)	0.00(+0.00)	40.89(-25.11)	0.00(+0.00)	

Table 4 shows the result of the ablation study for in-context learning with LLaVA-1.5. We repeated the experiment 10 times. The result shows that zero-shot does not yield different results throughout 10 repeats when the same hyperparameter and prompt are used for inference. For SIMPLE difficulty, the best mean F1 score comes from in-context learning for both MIMIC-CXR and IU-Xray datasets. Still, there is no clear trend of performance over the number of shots. In fact, for some of the trials with MIMIC-CXR, the performance of the model with more shots is lower than that for zero-shot. The increase in performance is also observed in COMPLEX difficulty. Similar to SIMPLE tasks, there is no clear association between the performance and the number of shots. The effect of in-context learning is higher in COMPLEX than in SIMPLE difficulty. Providing one example increases the performance in MIMIC-CXR SIMPLE by 3.5 and in IU-Xray SIMPLE by 3.62, while it increases the performance in COMPLEX setting in MIMIC-CXR and IU-Xray by 9.75 and 13.37 respectively.

**Table 4.** Ablation study for In-context learning. We repeated the experiment 10 times. The reported F1 score is the average of the 10 repeats, and the standard deviation is provided.

	MIMIC-CXR		IU-Xray	
# Shots	SIMPLE(F1)	COMPLEX(F1)	SIMPLE(F1)	COMPLEX(F1)
0	35.79±0.00	$0.00\pm0.00$	40.60±0.00	0.00±0.00
1	39.29±1.47	9.75±4.48	44.22±2.96	13.37±6.04
2	<b>39.78</b> ±1.27	13.98±5.75	39.55±8.62	12.81±6.02
3	35.04±9.45	<b>14.35</b> ±4.86	41.74±2.49	9.64±7.04
4	25.22±8.76	8.70±9.55	42.04±4.56	9.74±5.57
5	34.13±12.82	10.31±8.70	44.03±6.15	8.87±5.40
6	34.24±12.07	9.07±8.05	44.02±4.98	8.91±5.87
7	35.83±9.93	7.52±6.65	44.24±2.19	11.15±7.81
8	37.69±9.67	9.22±7.68	43.81±2.48	<b>13.93</b> ±8.71
9	35.64±10.47	7.87±5.92	<b>44.50</b> ±2.54	11.07±7.68
10	34.13±12.34	7.33±7.04	41.94±4.04	12.00±8.30

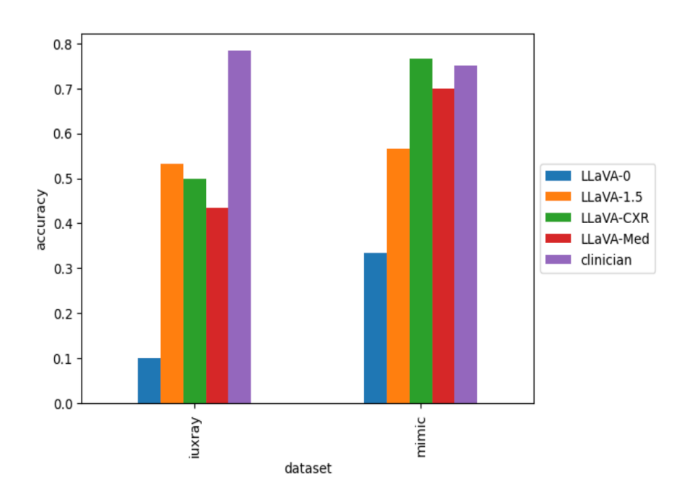


**Figure 5.** Accuracy of human evaluation in the SIMPLE setting.

#### **Human Evaluation Result**

Figure 5 shows the accuracy of the human evaluation for all the models and clinicians for the SIMPLE difficulty. The domain experts performed best in IU-Xray with 78.3% accuracy. In the order of accuracy, LLaVA-1.5, LLaVA-CXR, LLaVA-Med, and LLaVA-0 performed 53.3%, 50.0%, 43.3%, and 10.0% respectively. The accuracy gap between the best model, LLaVA-1.5, and clinicians was 25.0%. However, for the MIMIC-CXR dataset, LLaVA-CXR outperformed with an accuracy of 76.7%, surpassing domain experts at 75.0%. LLaVA-Med was slightly worse than domain experts with 70.0% accuracy. LLaVA-1.5 and LLaVA-0 performed relatively poorly, 56.7% and 33.3%, respectively. This result highlights the effect of fine-tuning large language and vision models in the target domain.

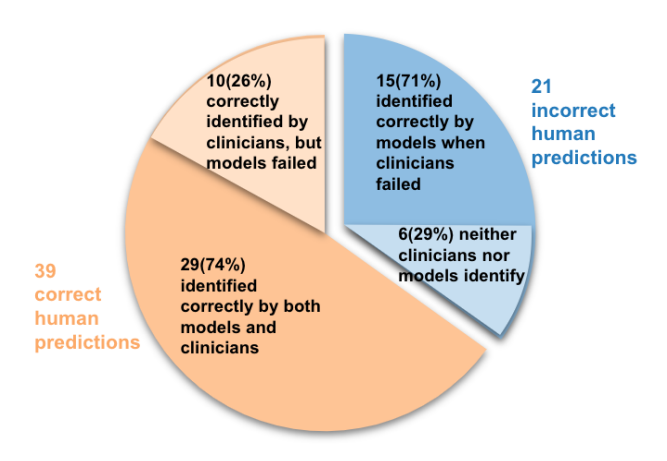


**Figure 6.** Vision LLMs can assist clinicians. The pie chart illustrates the human performance vs ensemble model performance. In 39 (65%) of the reports, both clinicians predicted correctly, whereas in 21 (35%) reports, one of the clinicians failed.

Further analysis of the human evaluation dataset reveals interesting findings indicating the feasibility of Vision LLMs as clinical assistants, as depicted in Figure 6. For this analysis, we used an ensemble of LLaVA models, hereafter referred to as **LLaVA-ensemble**, excluding LLaVA-0 to make an odd number of voting models. We used majority voting as well as logical OR operation to aggregate the responses from the three models. Figure 6 shows the result of the logical OR operation ensemble. In the total 60 examples, there was a subset of 21 samples (the big circle on the left in Figure 6), for each of which at least one domain expert failed to get the right answer. For this subset, **LLaVA-ensemble** was able to correctly check 15 (71.4%) reports. However, the majority voting aggregation had lower correct reports, 8 (38.1%) reports.

Figure 6 also demonstrates the performance of the models on the subset(n=39) in which both clinicians got the correctanswers. Out of these reports, LLaVA-ensemble correctly identified the existence of the mistakes in 29 reports (74.4%) regardless of the aggregation policy (voting and logical OR).

These results underscore the synergistic potential of LLaVA-ensemble as a clinical decision support tool, capable of rectifying oversights made by radiologists. The ensemble's ability to correctly identify the reports where errors eluded domain expert detection highlights its complementary role in enhancing diagnostic accuracy. Moreover, the comparison between aggregation techniques reveals that logical OR operation, by considering a positive prediction if at least one model responds positively, captures subtle errors that can be overlooked.

#### **DISCUSSION**

In exploring the usefulness of multimodal large language models (LLMs) in enhancing radiology report error-checking, our study reveals interesting findings across various evaluation approaches. The zero-shot evaluation results demonstrate the effectiveness of instruction tuning in the medical domain, enhancing the model's innate capacity for error-checking in the SIMPLE setting (Table 2). Notably, LLaVA-CXR emerges as the best-performing model for SIMPLE difficulty, highlighting proficiency in understanding radiographs without additional examples. The effectiveness of instruction tuning is also confirmed when we compare the result of LLaVA-Med and its baseline model LLaVA-0.

However, when the examples are provided for in-context learning, both fine-tuned models performed relatively poorly compared to their baseline models (Table 3). LLaVA-1.5 emerges as the most robust model, where providing examples for each choice consistently enhances performance. In contrast, LLaVA-Med performs worse than in-context learning in all scenarios. Further investigation is required to determine whether fine-tuning truly limits the model capacity of in-context learning. The ablation study on the LLaVA-1.5 model shows there is no clear relationship between the number of shots and performance. The effect of in-context learning is more pronounced in the COMPLEX difficulty cases, indicating its potential for addressing more intricate tasks. Regardless of the difficulty levels, the result confirms that adding more examples does not guarantee a performance boost. In fact, providing one example was enough for the desired performance boost (Table 4).

Zero-shot and Few-shot evaluation results highlight the importance of the backbone large language model. LLaVA-1.5 outperforms LLaVA-Med in all cases except the zero-shot COMPLEX setting. This is also confirmed by qualitative analysis (Figure 4). As the models

tested in this study are all based on a general domain LLM, a future study on vision and language models made from a medical LLM could provide insights into the importance of the backbone model.

The evaluation by expert clinicians provides valuable insights. Although the domain experts performed generally better than the models, the LLaVA-CXR model, which was fine-tuned on the MIMIC-CXR instruction dataset for error-checking, performed 1.67% better than humans in the MIMIC-CXR dataset. The detailed analysis of the human evaluation dataset also suggests the potential of Vision LLMs as valuable assistants in clinical settings. LLaVA-ensemble can correct mistakes overlooked by domain experts, showcasing the potential of this model as an assistant in clinical decision-making. Still, the fine-tuned model performed worse than humans with the unseen data format, the IU-Xray dataset, suggesting the need to add more public and custom data to fine-tune the model before it is implemented in hospital settings.

In addition, we recognize that our dataset may not fully replicate the complexities of real-world scenarios. A notable instance is the deidentification issue causing confusion or both the model and clinicians several text artifacts ('XXXX') to be left within the radiology reports in the evaluation dataset. This issue occasionally led to confusion for both the model and clinicians during decision-making as it could be difficult to fully exclude a 'substitute' error. This issue was particularly prominent in the IU X-ray dataset, potentially contributing to the observed variance in performance between the IU X-ray and MIMIC-CXR datasets in certain scenarios.

Clinicians observed that some synthetic errors, especially the 'insert' and 'substitute' types, appeared somewhat unrealistic in the evaluation dataset. In some cases, the errors seemed unnatural in real-world reports, except in rare voice dictation errors. Thus, these results may be particularly useful for voice recognition/dictation software errors in radiology reports.

Identifying 'remove' errors presents a challenge due to the inherent variability in the dataset's unstructured radiology reports. In this study, 'remove' errors were marked only when omitted information was considered crucial by the evaluator e.g. when a significant pneumothorax was not reported. However, this approach is inherently subjective, and what is deemed a non-error in one instance might be argued otherwise by another, especially in the absence of structured reporting guidelines. This highlights the ongoing issue of subjectivity in error identification within unstructured radiological assessments.

Furthermore, radiologists typically consider a range of contextual and clinical information, including input from colleagues and previous imaging studies, to form a comprehensive judgment of an image. Our evaluation process was limited in this regard, as it did not fully incorporate these additional data sources.

In future studies, it would be valuable to explore more on enhancing the explanatory capabilities of models analyzing chest X-rays. For example, to not only identify whether it has a mistake but also to provide detailed explanations of their interpretations. This would deepen our understanding of how these models perceive and interpret medical image, advancing the field of AI in diagnostic radiology.

# **CONCLUSION**

In conclusion, this research highlights the potential groundbreaking role of multimodal LLMs in radiology, emphasizing their value as assistants for radiologists. The study's thorough evaluation

and analysis, encompassing zero-shot, fine-tuning, and in-context learning, alongside human assessments, provide a comprehensive understanding of these models in chest X-ray error-checking. It underscores the strengths, limitations, and practical implications of the current multimodal LLMs, LLaVA models, paving the way for ongoing advancements. This research also created an error-checking benchmark dataset, the first of its kind. This will facilitate the research of a collaborative framework between AI models and medical professionals for enhancing diagnostic precision and operational efficiency in healthcare, thereby opening new avenues for AI-assisted medical imaging.

#### References

- 1. Dunnick NR, Langlotz CP. The radiology report of the future: a summary of the 2007 Intersociety Conference. Journal of the American College of Radiology. 2008 May 1;5(5):626-9.
- 2. Wallis A, McCoubrie P. The radiology report—are we getting the message across?. Clinical radiology. 2011 Nov 1;66(11):1015-22.
- 3. Cassar A, Holmes Jr DR, Rihal CS, Gersh BJ. Chronic coronary artery disease: diagnosis and management. InMayo Clinic Proceedings 2009 Dec 1 (Vol. 84, No. 12, pp. 1130-1146). Elsevier.
- 4. Radford A, Narasimhan K, Salimans T, Sutskever I. Improving language understanding by generative pre-training.
- 5. Radford A, Wu J, Child R, Luan D, Amodei D, Sutskever I. Language models are unsupervised multitask learners. OpenAI blog. 2019 Feb 24;1(8):9.
- 6. Brown T, Mann B, Ryder N, Subbiah M, Kaplan JD, Dhariwal P, Neelakantan A, Shyam P, Sastry G, Askell A, Agarwal S. Language models are few-shot learners. Advances in neural information processing systems. 2020;33:1877-901.
- 7. Ouyang L, Wu J, Jiang X, Almeida D, Wainwright C, Mishkin P, Zhang C, Agarwal S, Slama K, Ray A, Schulman J. Training language models to follow instructions with human feedback. Advances in Neural Information Processing Systems. 2022 Dec 6;35:27730-44.
- 8. Zhang Y, Ding DY, Qian T, Manning CD, Langlotz CP. Learning to summarize radiology findings. arXiv preprint arXiv:1809.04698. 2018 Sep 12.
- 9. Zhang Y, Wang X, Xu Z, Yu Q, Yuille A, Xu D. When radiology report generation meets knowledge graph. InProceedings of the AAAI Conference on Artificial Intelligence 2020 Apr 3 (Vol. 34, No. 07, pp. 12910-12917).
- 10. Xue Y, Xu T, Rodney Long L, Xue Z, Antani S, Thoma GR, Huang X. Multimodal recurrent model with attention for automated radiology report generation. InMedical Image Computing and Computer Assisted Intervention–MICCAI 2018: 21st International Conference, Granada, Spain, September 16-20, 2018, Proceedings, Part I 2018 (pp. 457-466). Springer International Publishing.
- 11. Brady AP. Error and discrepancy in radiology: inevitable or avoidable?. Insights into imaging. 2017 Feb;8:171-82.
- 12. Brady AP, Bello JA, Derchi LE, Fuchsjäger M, Goergen S, Krestin GP, Lee EJ, Levin DC, Pressacco J, Rao VM, Slavotinek J. Radiology in the era of value-based healthcare: a

- multi-society expert statement from the ACR, CAR, ESR, IS3R, RANZCR, and RSNA. Canadian Association of Radiologists Journal. 2021 May;72(2):208-14.
- 13. Yu F, Endo M, Krishnan R, Pan I, Tsai A, Reis EP, Fonseca EK, Lee H, Shakeri Z, Ng A, Langlotz C. Radiology Report Expert Evaluation (ReXVal) Dataset.
- 14. Johnson AE, Pollard TJ, Berkowitz SJ, Greenbaum NR, Lungren MP, Deng CY, Mark RG, Horng S. MIMIC-CXR, a de-identified publicly available database of chest radiographs with free-text reports. Scientific data. 2019 Dec 12;6(1):317.
- 15. Demner-Fushman D, Antani S, Simpson M, Thoma GR. Design and development of a multimodal biomedical information retrieval system. Journal of Computing Science and Engineering. 2012 Jun 30;6(2):168-77.
- 16. Wu H, Toti G, Morley KI, Ibrahim ZM, Folarin A, Jackson R, Kartoglu I, Agrawal A, Stringer C, Gale D, Gorrell G. SemEHR: A general-purpose semantic search system to surface semantic data from clinical notes for tailored care, trial recruitment, and clinical research. Journal of the American Medical Informatics Association. 2018 May;25(5):530-7.
- 17. Touvron H, Lavril T, Izacard G, Martinet X, Lachaux MA, Lacroix T, Rozière B, Goyal N, Hambro E, Azhar F, Rodriguez A. Llama: Open and efficient foundation language models. arXiv preprint arXiv:2302.13971. 2023 Feb 27.
- 18. Touvron H, Martin L, Stone K, Albert P, Almahairi A, Babaei Y, Bashlykov N, Batra S, Bhargava P, Bhosale S, Bikel D. Llama 2: Open foundation and fine-tuned chat models. arXiv preprint arXiv:2307.09288. 2023 Jul 18.
- 19. Liu H, Li C, Wu Q, Lee YJ. Visual instruction tuning. arXiv preprint arXiv:2304.08485. 2023 Apr 17.
- 20. Liu H, Li C, Li Y, Lee YJ. Improved baselines with visual instruction tuning. arXiv preprint arXiv:2310.03744. 2023 Oct 5.
- 21. Li C, Wong C, Zhang S, Usuyama N, Liu H, Yang J, Naumann T, Poon H, Gao J. Llava-med: Training a large language-and-vision assistant for biomedicine in one day. arXiv preprint arXiv:2306.00890, 2023 Jun.
- 22. Hu EJ, Shen Y, Wallis P, Allen-Zhu Z, Li Y, Wang S, Wang L, Chen W. Lora: Low-rank adaptation of large language models. arXiv preprint arXiv:2106.09685. 2021 Jun 17.
- 23. Rajbhandari S, Rasley J, Ruwase O, He Y. Zero: Memory optimizations toward training trillion parameter models. InSC20: International Conference for High Performance Computing, Networking, Storage and Analysis 2020 Nov 9 (pp. 1-16). IEEE.
- 24. Dao T, Fu D, Ermon S, Rudra A, Ré C. Flashattention: Fast and memory-efficient exact attention with io-awareness. Advances in Neural Information Processing Systems. 2022 Dec 6;35:16344-59.

# Appendix

**Table 5.** Important clinical concepts annotated by clinicians are randomly modified in the evaluation data.

Concept	Semantic type
Effusion pleural	Disease or Syndrome
Consolidation	Disease or Syndrome
Opacity	Finding
Atelectases	Pathologic Function
Wet Lung	Pathologic Function
Effusion	Pathologic Function
No gross lesions	Finding
Pneumonia	Disease or Syndrome
Congestion	Pathologic Function
Dropsy	Pathologic Function
Fracture rib	Injury or Poisoning
Opaque	Finding
Left lung base	Body Location or Region
Right lung base	Body Location or Region
Right lower lobe	Body Part, Organ, or Organ Component
Infection	Disease or Syndrome
Fracture	Injury or Poisoning
Thoracic aorta	Body Part, Organ, or Organ Component
Lobe	Body Part, Organ, or Organ Component
COPD NOS	Disease or Syndrome
Emphysema	Pathologic Function
Displaced fracture	Injury or Poisoning
H hernia	Disease or Syndrome
Pulmonary edema interstitial	Disease or Syndrome
right-sided pleural effusion	Pathologic Function
Both lungs	Body Part, Organ, or Organ Component
Drainage	Therapeutic or Preventive Procedure
left-sided pleural effusion	Pathologic Function

Infectious process	Pathologic Function
Pulmonary nodules	Finding
Lung nodule	Finding
Peribronchial cuffing	Finding
Right pneumothorax	Finding